Composite Structures 159 (2017) 44–52

Contents lists available at ScienceDirect

Composite Structures

journal homepage: www.elsevier.com/locate/compstruct

A novel invariant-based design approach to carbon fiber reinforced laminates

Jose Daniel D. Melo [a,*], Jing Bi [b], Stephen W. Tsai [c]

[a] Department of Materials Engineering, Federal University of Rio Grande do Norte, Campus Central, 3000, Natal, RN 59078-970, Brazil
[b] Dassault Systemes SIMULIA, 1301 Atwood Ave, Johnston, RI 02919, United States
[c] Department of Aeronautics & Astronautics, Stanford University, Durand Building, 496 Lomita Mall, Stanford, CA 94305-4035, United States

ARTICLE INFO

Article history:
Received 12 July 2016
Revised 17 September 2016
Accepted 19 September 2016
Available online 19 September 2016

Keywords:
Invariant-based design
Trace
Unit circle
Carbon fiber reinforced polymer

ABSTRACT

An invariant-based design procedure using trace-normalized plane stress stiffness matrix and unit circle failure criterion for carbon fiber reinforced polymer (CFRP) is presented and compared to the traditional design approach. Using the invariant-based design approach, the optimal stiffness-based layup solution is material independent and thus valid for any CFRP. Then, trace of the plane stress stiffness matrix is the only material property needed for strain scaling. Moreover, the unit circle failure criterion is invariant with respect to ply orientation and requires only the unidirectional longitudinal tensile and compressive strains-to-failure, which greatly simplifies testing. In this study, smooth and open-hole plates are evaluated using the traditional design approach and invariant-based design procedures. The results show that the invariant-based design approach greatly simplifies the design procedure of CFRP structural components.

1. Introduction

Because of their superior properties, carbon fiber reinforced polymer (CFRP) composites are the material of choice for a variety of structural applications, which demand high strength- and modulus-to-weight ratio and corrosion resistance. However, the inherent anisotropy of these materials – fundamental to design flexibility and to their superior properties – makes their mechanical characterization complex, costly and time consuming. For unidirectional plies under in-plane loading, there are four independent stiffness parameters to be measured; *i.e.*, longitudinal, transverse and shear moduli and Poisson's ratio; and five strengths for criteria such as Tsai-Wu [1]; *i.e.*, longitudinal and transverse tensile and compressive, and shear. Likewise, finding an optimal design of composite laminates is significantly complicated due to the large number of possible combinations of material properties and stacking sequences.

Numerous studies for design optimization of composite structural components have been presented in the literature [2–14]. While some optimization approaches may assume a fixed geometry (topology) of the component and concentrate the effort on optimizing laminate properties, others focus on both optimum layup configurations and thickness profiles. Design constraints may include maximum stiffness and minimum weight [3] or stiffness and aeroelastic requirements [4,5]. In some cases, the layup is fixed and only thickness optimization is performed [15–17]. In other cases, the focus is mainly placed on stacking sequence optimization [18–26], sometimes with a fixed number of ply orientations [27–29]. Considering the specific material properties for each optimization study, scaling for different materials is usually not possible, and thus, the solution is material specific.

Recently, an invariant-based approach was proposed to describe elastic properties and failure of carbon fiber reinforced composite laminates [30]. The plane stress stiffness matrix components have been shown to be invariant when normalized by its trace. Thus, a "master ply" was defined using trace-normalized stiffness components to describe the stiffness properties of all CFRPs. A unit circle was also proposed as an invariant failure envelope in strain space to all CFRPs [31]. The criterion is based on uniaxial tensile and compressive strains-to-failure of a unidirectional ply. Thus, the number of independent parameters to be determined is greatly reduced as compared to typical failure criteria currently used. In addition, these tests are simpler to perform when compared to shear tests, normally required in most failure criteria.

The purpose of the present work is to describe a design procedure using the invariant-based approach to the optimal design of

* Corresponding author.
E-mail address: jddmelo@gmail.com (J.D.D. Melo).

http://dx.doi.org/10.1016/j.compstruct.2016.09.055
0263-8223/

structural components made of carbon fiber reinforced composite materials and compare it to a traditional design method.

2. Background

Carbon fiber tapes have been shown to share common stiffness properties if they are normalized by their respective trace of the plane stress stiffness matrix, where *Tr* [*Q*] is given by Eq. (1) [30,32].

$$\mathrm{Tr}[Q] = Q_{xx} + Q_{yy} + 2Q_{ss} = Q_{11} + Q_{22} + 2Q_{66} \quad (1)$$

In Table 1, trace-normalized stiffness factors are shown for fifteen different carbon fiber composites [32]. Although the elastic constants for the various materials are very different, their trace-normalized properties are very similar. Thus, their mean values have been used to define a "master ply".

The master ply properties shown in Table 1 are valid for unidirectional CFRP tapes. For glass/polymer composites, the fiber dominance on ply trace is less than that of carbon composites, due to the much lower elastic modulus of glass fibers as compared to carbon fibers. Also, fiber volume fractions in these materials are normally lower than those of typical CFRPs. Thus, there is a greater variation in trace normalized stiffness components among different glass/polymer composites and a master-ply may not be a good representation of these materials.

In-plane and flexural laminate stiffness of composite laminates – [A] and [D] – can be normalized according to Eq. (2) so that material and geometry contributions are separated and [A*] and [D*] will have the same units.

$$[A^*] = \frac{1}{h}[A]$$
$$[D^*] = \frac{12}{h^3}[D] \quad (2)$$

The terms of [A*] are not dependent on stacking sequence, but those of [D*] are. However, the traces of both [A*] and [D*] have the same value, thus invariant to stacking sequence as shown in Fig. 1, where stiffness components are presented as a function of ply orientation for a [0/+θ/−θ] laminate. These trace values are also the same as trace [Q].

In case master ply properties are used, all stiffness properties are trace normalized. Thus, the curves will be valid not only for a specific material as in Fig. 1, but to any CFRP composed of UD plies (Fig. 2). The curves for a specific material can be obtained if the stiffness components are multiplied by trace [Q] for that material.

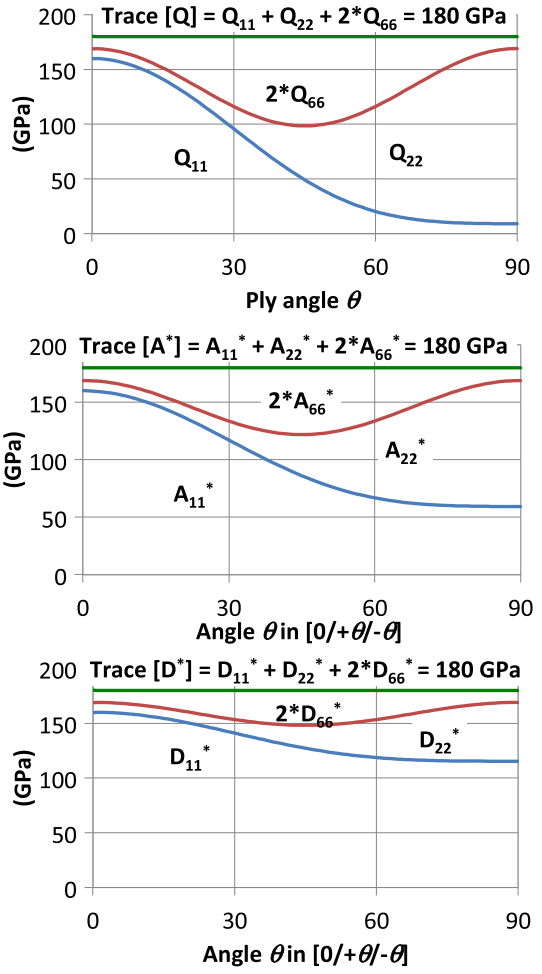

Fig. 1. Unidirectional ply and in-plane and flexural stiffness components as a function of ply orientation for IM7/8552.

Thus, with trace normalized stiffness components, design optimization is more efficient since once the best laminate is defined, the solution is general, not limited to a specific material.

Table 1
Elastic properties and trace normalized plane stress stiffness components for various carbon composites.

Material	E_x (GPa)	E_y (GPa)	ν_x	E_s (GPa)	Q^*_{xx}	Q^*_{yy}	Q^*_{xy}	Q^*_{ss}	Tr (GPa)
IM6/epoxy	203	11.20	0.32	8.40	0.8791	0.0485	0.0155	0.0362	232
IM7/977-3	191	9.94	0.35	7.79	0.8825	0.0459	0.0161	0.0358	218
T300/5208	181	10.30	0.28	7.17	0.8805	0.0501	0.0140	0.0347	206
IM7/MTM45	175	8.20	0.33	5.50	0.9014	0.0422	0.0139	0.0282	195
T800/Cytec	162	9.00	0.40	5.00	0.8955	0.0497	0.0199	0.0274	183
IM7/8552	159	8.96	0.32	5.50	0.8888	0.0501	0.0160	0.0306	180
T800S/3900	151	8.20	0.33	4.00	0.9034	0.0491	0.0162	0.0238	168
T300/F934	148	9.65	0.30	4.55	0.8878	0.0579	0.0174	0.0271	168
T700 C-Ply 64	141	9.30	0.30	5.80	0.8713	0.0575	0.0172	0.0356	163
AS4/H3501	138	8.96	0.30	7.10	0.8567	0.0556	0.0167	0.0438	162
T650/epoxy	139	9.40	0.32	5.50	0.8724	0.0590	0.0189	0.0343	160
T4708/MR60H	142	7.72	0.34	3.80	0.9029	0.0491	0.0167	0.0240	158
T700/2510	126	8.40	0.31	4.20	0.8827	0.0588	0.0182	0.0292	144
AS4/MTM45	128	7.93	0.30	3.65	0.8939	0.0554	0.0166	0.0253	144
T700 C-Ply 55	121	8.00	0.30	4.70	0.8746	0.0578	0.0173	0.0338	139
Std dev	24.6	1.0	0.029	1.5	0.0132	0.0053	0.0016	0.0056	
Coeff var%	16.0	10.9	9.0	27.2	1.5	10.1	9.6	17.9	
Master ply					0.8849	0.0525	0.0167	0.0313	1.0

Note: Q^*_{ij} are the trace-normalized plane stress stiffness components.

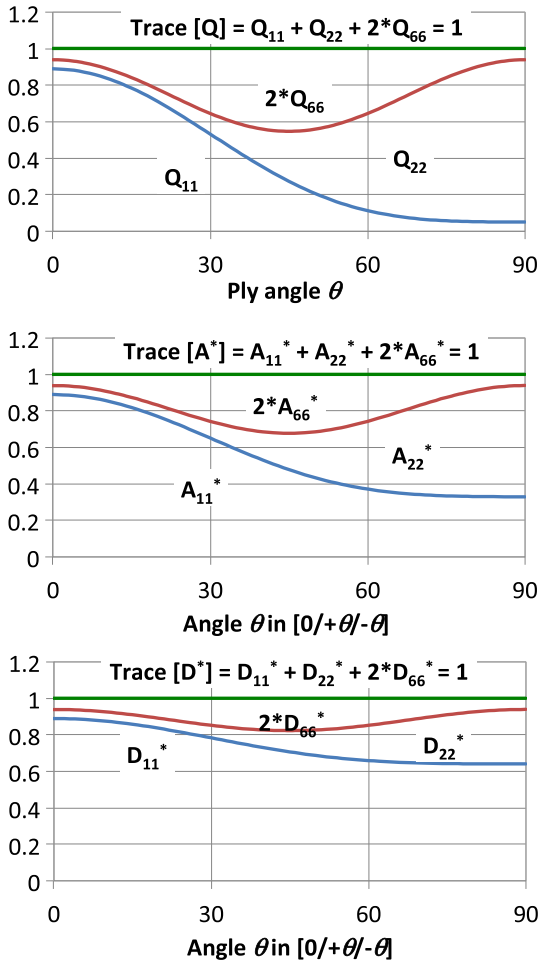

Fig. 2. Unidirectional ply and in-plane and flexural stiffness components as a function of ply orientation for "master ply".

3. Designing with trace

Most structures are designed using finite element analysis software. These programs require material properties for simulation. The trace-normalized elastic properties for a master ply are shown in Table 2, based on the components of trace normalized plane stress stiffness matrix given in Table 1.

It is observed in Table 2 that the longitudinal elastic modulus E_x^* for CFRP plies is approximately 88% of trace [Q]. Thus, for a given CFRP material, Tr [Q] can be determined from the longitudinal elastic modulus as shown in Eq. (3).

$$Tr[Q] = \frac{E_x}{0.8796} \tag{3}$$

The invariant-based approach for design using master ply trace-normalized elastic properties (Table 2) is shown in Fig. 1. The same figure shows the traditional approach for comparison.

As shown in Fig. 3, an optimized design for a given set of loads is only valid for a specific material when the traditional design approach is used. Thus, if a material is changed, the optimization procedure needs to be conducted again. In contrast, the trace-based optimized solution is valid for any CFRP. Once the optimized solution is determined for the master ply, trace can be used as the scaling factor for the determination of strains.

Table 2
Elastic constants for a master ply.

Material	E_x^*	E_y^*	ν_x	E_s^*
Master Ply	0.8796	0.0522	0.3181	0.0313

Note: E_x^*, E_y^*, E_s^*, are the ply longitudinal, transverse and shear moduli normalized by trace, respectively, and ν_x is the major Poisson's ratio.

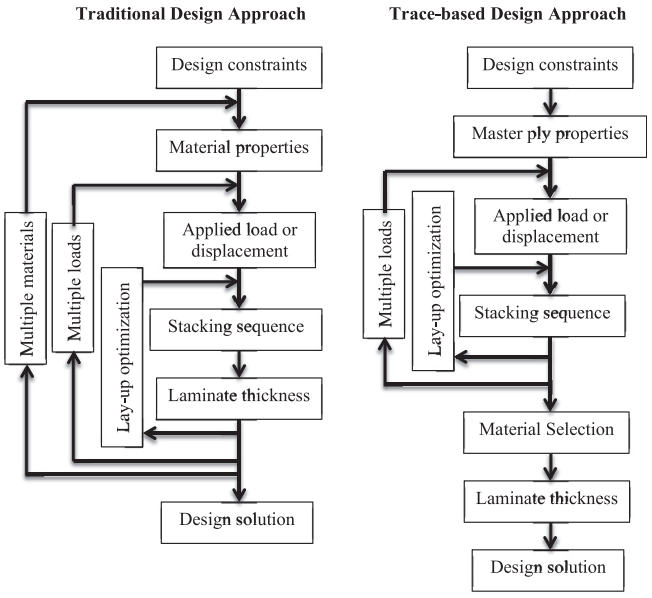

Fig. 3. Flow chart with the traditional and trace-based sizing approaches.

Strength calculation needs only to be conducted after a material has been selected. Then, the calculation can be greatly simplified if the unit circle failure criterion is used [31]. In this case, only longitudinal tensile and compressive strengths are used in addition to the longitudinal elastic modulus. The unit circle failure criterion is given in Fig. 4.

The following example cases illustrate the use of the invariant-based approach for design. The material properties used are given in Table 1.

3.1. In-plane load

For this example, the design constraints considered are that any strain component must be smaller than 5.0×10^{-3} in addition to a

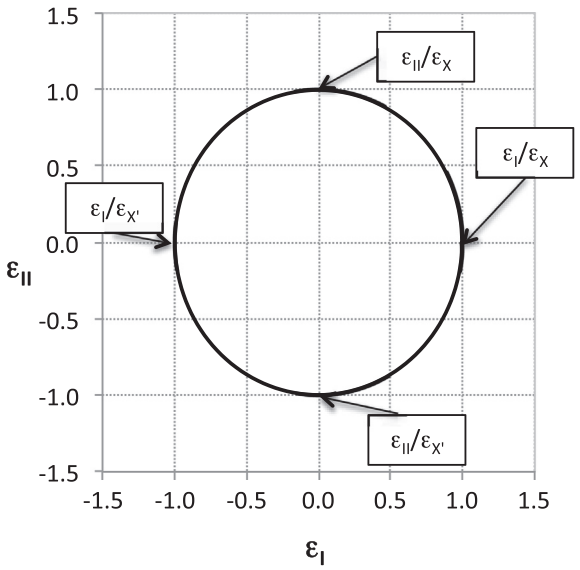

Fig. 4. Unit circle failure envelope.

Table 3
Load cases and lay-ups considered for design.

Load Case $\{N_1, N_2, N_6\}$ (MN/m)	$[0/\pm45/90]_{2s}$	$[0_5/\pm45/90]_s$	$[0/\pm45_3/90]_s$
{0.5, 0.0, 0.0}	x	x	x
{0.5, 0.2, 0.0}	x	x	x
{0.5, −0.2, 0.0}	x	x	x
{−0.5, 0.0, 0.0}	x	x	x
{0.5, 0.0, 0.1}	x	x	x

safety factor of at least 2.0 (failure index of 0.5). Failure index will be calculated for the unit circle failure criterion.

The materials to be considered are T700 C-Ply 55, AS4/H3501 and T300/5208. Four load cases must be considered, as shown in Table 3. In addition, three laminates with sixteen plies each will be evaluated: $[\pi/4]_{2s}$, a hard $[0_5/\pm45/90]_s$ and a soft $[0/\pm45_3/90]_s$. For all materials ply thickness is 125 μm and matrix degradation factor was assumed as $E_m^* = 0.15$.

For the unit circle failure criterion, only the longitudinal tensile and compressive strengths are needed, in addition to the longitudinal elastic modulus. The properties X, X′ and E_x used for these three materials are shown in Table 4. Other strength parameters and degraded elastic properties for these three materials are also shown in Table 4.

3.2. Open hole – using master ply for stress concentration

Exact solutions for practical problems of homogeneous anisotropic materials such as stress concentration around open holes have been developed in the past [33]. Although exact solutions are limited when boundary conditions are complex, they provide the best source of validation for numerical solutions. They have no mesh dependency or convergence issue.

For anisotropic materials under plane stress, the stress distribution around a notch depends on the elastic constants of the material. For laminated composites, the effective constants of the laminate shall be used. Such direct substitution makes the trace-based approach very convenient for these calculations. Thus, the use of the trace-based approach for both exact and numerical solutions will be discussed.

For the exact solution, the equations for the stress distribution in an orthotropic plate with a circular hole under tension in the principal direction are used (Fig. 5). The stresses are calculated at points A and A_1 (Fig. 5), at the ends of the diameter in the direction parallel to the applied forces, according to Eq. (4).

$$\sigma_\theta = -\frac{p}{K} \tag{4}$$

And at points B and B_1 (Fig. 5), at the ends of the diameter perpendicular to the forces, the stress is given by Eq. (5).

$$\sigma_\theta = p(1+N) \tag{5}$$

where:

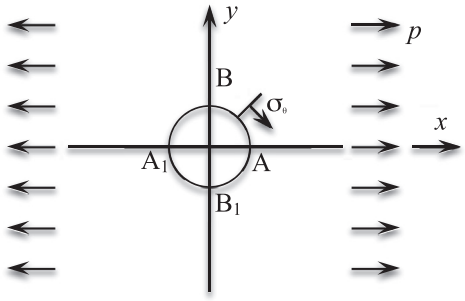

Fig. 5. Orthotropic plate with a circular hole under tension [33].

$$K = \sqrt{\frac{E_1}{E_2}}$$
and
$$N = \sqrt{2\left(\sqrt{\frac{E_1}{E_2}} - \nu_1\right) + \frac{E_1}{E_6}} \tag{6}$$

Thus, the stress concentration factors in Eqs. (4) and (5) are, respectively,

$$SCF_A = -\frac{1}{K} \tag{7}$$

$$SCF_B = N + 1 \tag{8}$$

These stress concentration factors will be calculated for three laminates – $[\pi/4]_{2s}$, hard $[0_5/\pm45/90]_s$ and soft $[0/\pm45_3/90]_s$ – using master ply properties and also the same materials considered in the previous example: T700 C-Ply 55, AS4/H3501 and T300/5208.

3.3. Open hole – using FEA for strength

To illustrate the use of the invariant-based approach for design, a Finite Element Analysis – FEA is also performed for the in-plane load and open hole problems. FEA has been widely used for practical engineering problems for its capability of solving boundary value problems with complex geometry, material, loading and boundary conditions. In this study, a commercial FEA software package – Abaqus/Standard – was used to solve the in-plane load and open hole boundary value problems.

A mesh convergence study was first carried out for the open hole problem with isotropic material for which theoretical solutions are well known. Then, the composite plate was modeled with composite shell formulation in Abaqus/Standard. A quarter of the open hole plate was modeled with symmetric boundary conditions. Smeared layers option with general shell section was used to eliminate the stacking sequence effect and obtain the laminate stiffness matrix. Other prediction approaches to model the effect of notches on strength of composite laminates have been described in the literature, in some cases showing remarkable agreement with experimental data [34,35]. However, improvements in

Table 4
Longitudinal strengths and elastic modulus for three CFRPs.

Material	E_x	E_y	ν_x	E_s	X	X′	Y	Y′	S
	Intact (Degraded)								
T700 C-Ply 55	121	8.00 (1.61)	0.30 (0.045)	4.7 (0.88)	2530	1669	66	220	93
AS4/H3501	138	8.96 (2.17)	0.30 (0.045)	7.10 (1.30)	1447	1447	52	206	93
T300/5208	181	10.30 (2.51)	0.28 (0.042)	7.17 (1.48)	1500	1500	40	246	68

Note: E_x, E_y, E_s, and ν_x are the longitudinal, transverse and shear moduli and major Poisson's ratio, respectively; X, X′, Y, Y′ and S are the longitudinal and transverse tensile and compressive and shear strengths, respectively. Elastic moduli in (GPa) and strengths in (MPa). $F_{xy}^* = -0.5$ for intact plies and $F_{xy}^* = -0.075$ for degraded plies. $E_m = 3.40$ GPa for all materials. Degraded moduli are calculated using micromechanics relations.

Table 5
Strains of CFRP laminates under various load cases.

Load Case $\{N_1, N_2, N_6\}$ (MN/m)	$[0/\pm45/90]_{2s}$ $\{\varepsilon_1, \varepsilon_2, \varepsilon_6\}$ (10^{-3})	$[0_5/\pm45/90]_s$ $\{\varepsilon_1, \varepsilon_2, \varepsilon_6\}$ (10^{-3})	$[0/\pm45_3/90]_s$ $\{\varepsilon_1, \varepsilon_2, \varepsilon_6\}$ (10^{-3})
T700 C-Ply 55			
{0.5, 0.0, 0.0}	{5.34, −1.62, 0.00}	{2.98, −0.90, 0.00}	{7.37, −3.66, 0.00}
{0.5, 0.2, 0.0}	{4.69, 0.51, 0.00}	{2.62, 2.56, 0.00}	{5.91, −0.71, 0.00}
{0.5, −0.2, 0.0}	{5.98, −3.76, 0.00}	{3.34, −4.37, 0.00}	{8.83, −6.61, 0.00}
{−0.5, 0.0, 0.0}	{−5.34, 1.62, 0.00}	{−2.98, 0.90, 0.00}	{−7.37, 3.66, 0.00}
{0.5, 0.0, 0.1}	{5.34, −1.62, 2.78}	{2.98, −0.90, 4.41}	{7.37, −3.66, 2.03}
AS4/H3501			
{0.5, 0.0, 0.0}	{4.56, −1.30, 0.00}	{2.59, −0.74, 0.00}	{6.02, −2.76, 0.00}
{0.5, 0.2, 0.0}	{4.04, 0.53, 0.00}	{2.30, 2.26, 0.00}	{4.92, −0.35, 0.00}
{0.5, −0.2, 0.0}	{5.08, −3.12, 0.00}	{2.89, −3.74, 0.00}	Fail
{−0.5, 0.0, 0.0}	{−4.56, 1.30, 0.00}	{−2.59, 0.74, 0.00}	{−6.02, 2.76, 0.00}
{0.5, 0.0, 0.1}	{4.56, −1.30, 2.34}	{2.59, −0.74, 3.51}	{6.02, −2.76, 1.76}
T300/5208			
{0.5, 0.0, 0.0}	{3.59, −1.06, 0.00}	{1.99, −0.59, 0.00}	{4.93, −2.41, 0.00}
{0.5, 0.2, 0.0}	{3.16, 0.37, 0.00}	{1.76, 1.79, 0.00}	{3.97, −0.43, 0.00}
{0.5, −0.2, 0.0}	{4.01, −2.50, 0.00}	{2.23, −2.96, 0.00}	Fail
{−0.5, 0.0, 0.0}	{−3.59, 1.06, 0.00}	{−1.99, 0.59, 0.00}	{−4.93, 2.41, 0.00}
{0.5, 0.0, 0.1}	{3.59, −1.06, 1.86}	{1.99, −0.59, 2.94}	{4.93, −2.41, 1.36}

accuracy are normally associated with increased complexity and additional properties required.

A shell edge load of 100 N/mm was applied at the right side edge with total plate thickness of 2 mm. Stress concentration factors for the open hole problem were calculated using the same laminates and materials considered for the exact solutions. In addition, failure analyses using FEA were also performed considering four load cases. A post processing python script was written and failure indices for all laminates and load cases were calculated using unit circle and Tsai-Wu failure criteria.

Table 6
Failure indices of CFRP laminates under various load cases.

Load Case $\{N_1, N_2, N_6\}$ (MN/m)	$[0/\pm45/90]_{2s}$ k	$[0_5/\pm45/90]_s$ k	$[0/\pm45_3/90]_s$ k
T700 C-Ply 55			
{0.5, 0.0, 0.0}	0.32	0.16	0.61
{0.5, 0.2, 0.0}	0.25	0.20	0.37
{0.5, −0.2, 0.0}	0.45	0.41	0.88
{−0.5, 0.0, 0.0}	0.45	0.23	0.74
{0.5, 0.0, 0.1}	0.34	0.29	0.61
AS4/H3501			
{0.5, 0.0, 0.0}	0.52	0.27	0.90
{0.5, 0.2, 0.0}	0.44	0.36	0.62
{0.5, −0.2, 0.0}	0.67	0.52	Fail
{−0.5, 0.0, 0.0}	0.52	0.27	0.90
{0.5, 0.0, 0.1}	0.56	0.44	0.91
T300/5208			
{0.5, 0.0, 0.0}	0.51	0.26	0.88
{0.5, 0.2, 0.0}	0.42	0.34	0.60
{0.5, −0.2, 0.0}	0.65	0.50	Fail
{−0.5, 0.0, 0.0}	0.51	0.26	0.88
{0.5, 0.0, 0.1}	0.54	0.43	0.89

4. Results and discussion

4.1. In-plane load

First, the traditional design was used for the calculation of strains and failure indices. In this case, the strains for each lay up and load case are calculated for a specific material. The results are shown in Table 5.

For each material, lay up and load case, the failure index (k) was determined based on the unit circle criterion. The results are shown in Table 6.

Therefore, based on the design constraints, the laminate that will best fit the requirements is the hard laminate $[0_5/\pm45/90]_s$ made from T700 C-Ply 55.

Now, if the same problem is solved using the trace-based approach, the strains are calculated for each laminate and applied load considering the master ply. The solution is shown in Table 7.

The solution in Table 7 applies to the same laminates made of any UD CFRP. It is clear that the hard laminate $[0_5/\pm45/90]_s$ results in the smallest strains and thus should be selected. The material selection can start by that material of smallest trace. In order to get the strains for a given material, the strains for the master ply can be divided by the trace of that material. For instance, if T700 C-Ply 55 is selected, Trace [Q] = 139 GPa. Then, the strains for this material can be determined if the strains in Table 7 are divided by 139 GPa, as shown in Table 8. In Table 8, the strains calculated

Table 7
Strains of master ply laminates under various load cases.

Load Case $\{N_1, N_2, N_6\}$ (MN/m)	$[0/\pm45/90]_{2s}$ $\{\varepsilon_1, \varepsilon_2, \varepsilon_6\}$ $(10^{-3}$ GPa)	$[0_5/\pm45/90]_s$ $\{\varepsilon_1, \varepsilon_2, \varepsilon_6\}$ $(10^{-3}$ GPa)	$[0/\pm45_3/90]_s$ $\{\varepsilon_1, \varepsilon_2, \varepsilon_6\}$ $(10^{-3}$ GPa)
Master ply			
{0.5, 0.0, 0.0}	{743.31, −228.30, 0.00}	{411.21, −126.85, 0.00}	{1038.99, −523.97, 0.00}
{0.5, 0.2, 0.0}	{652.00, 69.03, 0.00}	{360.46, 360.63, 0.00}	{829.40, −108.38, 0.00}
{0.5, −0.2, 0.0}	{834.63, −525.62, 0.00}	{461.95, −614.34, 0.00}	{1248.58, −939.57, 0.00}
{−0.5, 0.0, 0.0}	{−743.31, 228.30, 0.00}	{−411.21, 126.85, 0.00}	{−1038.99, 523.97, 0.00}
{0.5, 0.0, 0.1}	{743.31, −228.30, 388.64}	{411.21, −126.85, 625.19}	{1038.99, −523.97, 281.96}

Table 8
Strains of $[0_5/\pm45/90]_s$ T700 C-Ply 55 under five load cases calculated using master ply and actual material properties.

Load Case $\{N_1, N_2, N_6\}$ (MN/m)	$[0_5/\pm45/90]_s$ $\{\varepsilon_1, \varepsilon_2, \varepsilon_6\}$ (10^{-3}) Calculated from master ply and trace	$[0_5/\pm45/90]_s$ $\{\varepsilon_1, \varepsilon_2, \varepsilon_6\}$ (10^{-3}) Calculated using actual material properties
{0.5, 0.0, 0.0}	{2.96, −0.91, 0.00}	{2.98, −0.90, 0.00}
{0.5, 0.2, 0.0}	{2.59, 2.59, 0.00}	{2.62, 2.56, 0.00}
{0.5, −0.2, 0.0}	{3.32, −4.42, 0.00}	{3.34, −4.37, 0.00}
{−0.5, 0.0, 0.0}	{−2.96, 0.91, 0.00}	{−2.98, 0.90, 0.00}
{0.5, 0.0, 0.1}	{2.96, −0.91, 4.50}	{2.98, −0.90, 4.41}

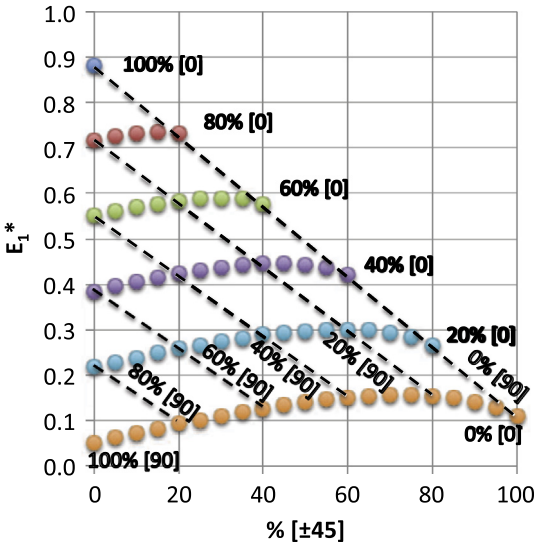

Fig. 6. Carpet plot for the longitudinal Young's modulus of a [π/4] family using master ply properties.

directly from material properties in Table 5 are also shown for comparison.

As it can be seen in Table 8, the strains calculated using the trace-based approach are very similar to those calculated using all elastic properties.

Since the material of smallest trace have met the stiffness criterion for the hard laminate $[0_5/\pm45/90]_s$, the failure criterion needs to be verified only for this specific material and laminate. The process for the verification of strength is the same as shown in Table 6 and need not to be repeated here.

The trace-based design approach can be extended to carpet plots. Carpet plots are very useful to stiffness-based designs. In Fig. 6, a carpet plot is shown for the longitudinal Young's modulus of a family of [π/4] balanced laminates using master ply properties. The same plot can be used for the transverse modulus. Since master ply properties were considered, this carpet plot is valid for all CFRPs. The Young's modulus for a specific laminate and material can be obtained if the normalized value is multiplied by the corresponding material trace. Thus, using trace, only one universal carpet plot is needed, instead of one for every material. In addition, the trace-based carpet plot is not sensitive to environmental conditions in cold-dry and hot-wet. Just need to get trace at the respective conditions.

4.2. Open hole – using master ply for stress concentration

The calculated stress concentration factors for the stresses at the ends of the diameter parallel and perpendicular to the force direction are shown in Table 9. The results include the three materials evaluated and also the master ply.

Table 9
Stress concentration factors for open hole plate under tensile stress.

Laminate	K	N	$-\frac{1}{K}$	$N+1$
T700 C-Ply 55				
$[0/\pm45/90]_{2s}$	1.00	2.00	−1.00	3.00
$[0_5/\pm45/90]_s$	1.70	3.23	−0.59	4.23
$[0/\pm45_3/90]_s$	1.00	1.54	−1.00	2.54
AS4/H3501				
$[0/\pm45/90]_{2s}$	1.00	2.00	−1.00	3.00
$[0_5/\pm45/90]_s$	1.71	3.11	−0.59	4.11
$[0/\pm45_3/90]_s$	1.00	1.60	−1.00	2.60
T300/5208				
$[0/\pm45/90]_{2s}$	1.00	2.00	−1.00	3.00
$[0_5/\pm45/90]_s$	1.73	3.29	−0.58	4.29
$[0/\pm45_3/90]_s$	1.00	1.55	−1.00	2.55
Master ply				
$[0/\pm45/90]_{2s}$	1.00	2.00	−1.00	3.00
$[0_5/\pm45/90]_s$	1.72	3.23	−0.58	4.23
$[0/\pm45_3/90]_s$	1.00	1.53	−1.00	2.53

As it can be seen in Table 9, stress concentration factors calculated using master ply are very similar to those calculated for each material. Therefore, master ply properties can be used with good accuracy for the calculation of stress concentration factors of open hole orthotropic plates.

The combined stress effects of notched strength as assumed to follow the same as those of smooth specimen strength. The implicit assumption is that the reduction in the uniaxial strength in tension and compression can be adequately represented by some strain reduction factor, and the effect under combined stress is carried over the same way.

4.3. Open hole – using FEA for strength

Stress concentration factors at the ends of the hole diameter parallel and perpendicular to the force direction obtained from FEA analyses are shown in Table 10. The results include the same three materials and the master ply evaluated in Table 9. A good correlation is observed between the stress concentration factors presented in Tables 10 and 9.

Fig. 7 illustrates the determination of the stress concentration factors using FEA. The figure shows stress components S11 and S22, in directions parallel and perpendicular to the applied load,

Table 10
Stress concentration factors for open hole plate under tensile stress from FEA analysis.

Laminate	$-\frac{1}{K}$	$N+1$
T700 C-Ply 55		
$[0/\pm45/90]_{2s}$	−1.02	3.01
$[0_5/\pm45/90]_s$	−0.60	3.98
$[0/\pm45_3/90]_s$	−1.03	2.62
AS4/H3501		
$[0/\pm45/90]_{2s}$	−1.02	3.01
$[0_5/\pm45/90]_s$	−0.59	4.29
$[0/\pm45_3/90]_s$	−1.04	2.46
T300/5208		
$[0/\pm45/90]_{2s}$	−1.02	3.01
$[0_5/\pm45/90]_s$	−0.60	3.98
$[0/\pm45_3/90]_s$	−1.03	2.63
Master Ply		
$[0/\pm45/90]_{2s}$	−1.02	3.01
$[0_5/\pm45/90]_s$	−0.60	4.01
$[0/\pm45_3/90]_s$	−1.03	2.61

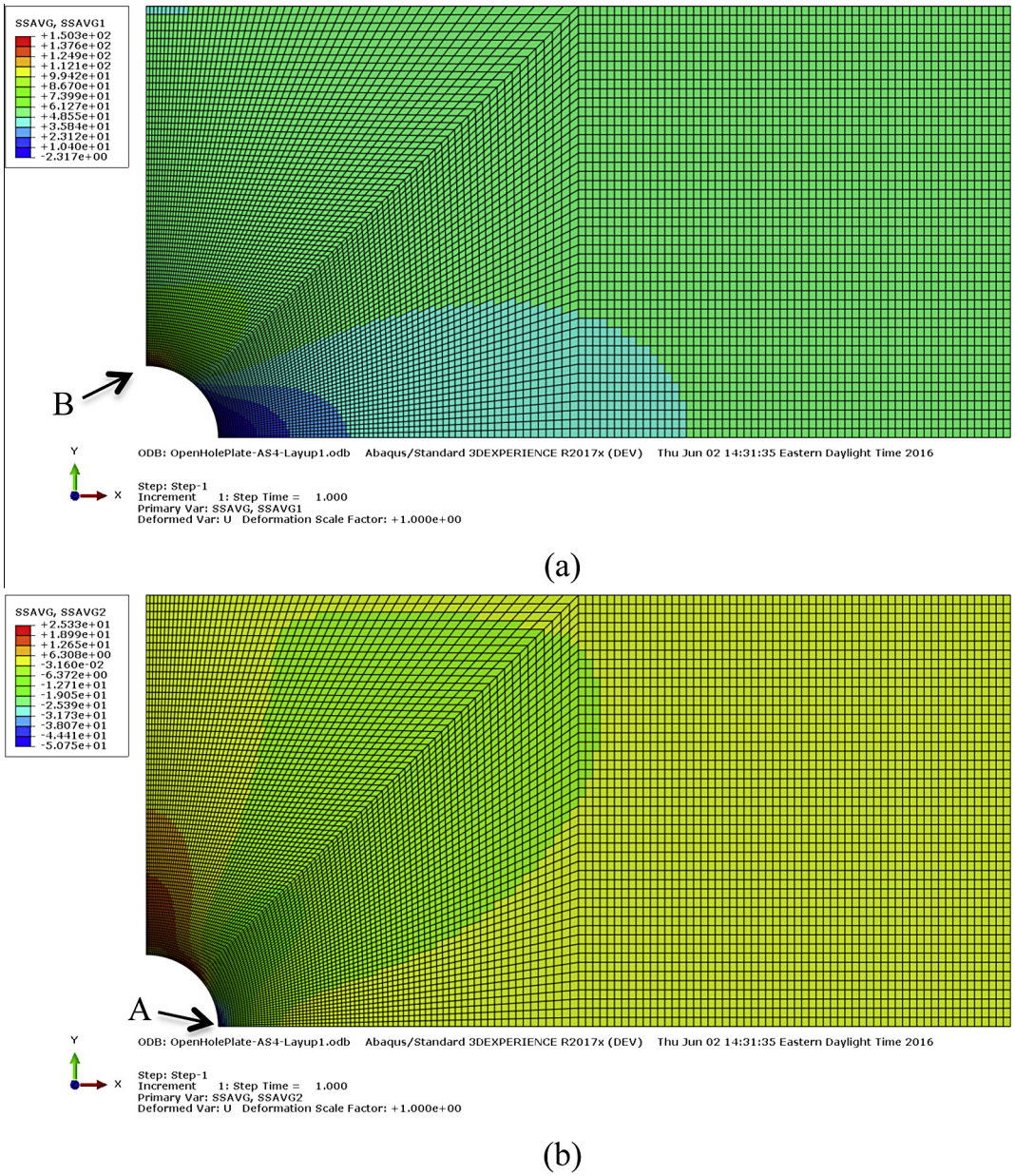

Fig. 7. Stress components at the hole edge: (a) S11 at point B, and (b) S22 at point A.

respectively, for AS4/H3501 with laminate $[0/\pm45/90]_{2s}$. Far field S11 is 50 MPa, corresponding to the applied pressure. S11 at point B (Fig. 5) is 150.292 MPa and S22 at point A (Fig. 5) is −50.7517 MPa. Thus, the corresponding stress concentration factors are $(N+1) = 3.01$ and $(-1/K) = -1.02$.

Failure analyses using FEA were also performed for the open hole CFRP laminates considering various load cases. Failure indices for all laminates and load cases are listed in Table 11 considering unit circle (U-C) and Tsai-Wu (T-W) failure criteria. Failure indices were determined considering the maximum value over the laminate. Laminate failure occurs when failure index reaches 1. It is shown in Table 11 that, in general, the unit circle failure criterion is more conservative than Tsai-Wu. As shown in Table 11, for some CFRP materials, failure indices based on unit circle can be slightly smaller as compared to those using Tsai-Wu, on specific areas of the failure envelope. This is due to the fact that matrix controlled strengths – Y, Y′ and S – which may affect the shape of the minimum inner failure envelope in strain space generated using Tsai-Wu, are not used to generate the unit circle. However, in these cases, the difference between the two failure criteria is small or negligible when compared to data scatter commonly found in strength data.

An example output contour plot of failure index (k) is shown in Fig. 8 for AS4/H3501 $[0/\pm45/90]_{2s}$, load case 1: $\{N_1, N_2, N_6\} = \{0.25, 0.0, 0.0\}$.

5. Conclusions

This work presented a design procedure using the invariant-based approach to the optimal design of structural components made of carbon fiber reinforced composite materials and compared it to the traditional design approach. Strains and failure indices were determined for laminated plates using invariants and also the traditional design. With the master ply concept, each laminate

Table 11
Failure indices (k) based on Unit Circle and Tsai-Wu failure criteria for open hole CFRP laminates under various load cases from FEA analyses.

Load Case $\{N_1, N_2, N_6\}$ (MN/m)	$[0/\pm45/90]_{2s}$ k		$[0_5/\pm45/90]_s$ k		$[0/\pm45_3/90]_s$ k	
	U-C	T-W	U-C	T-W	U-C	T-W
T700 C-Ply 55						
{0.25, 0.0, 0.0}	0.47	0.42	0.42	0.30	0.75	0.54
{0.25, 0.1, 0.0}	0.41	0.36	0.39	0.25	0.62	0.45
{0.25, −0.1, 0.0}	0.54	0.47	0.67	0.35	0.87	0.63
{−0.25, 0.0, 0.0}	0.66	0.68	0.55	0.49	0.92	0.93
AS4/H3501						
{0.25, 0.0, 0.0}	0.78	0.72	0.66	0.53	1.12	0.91
{0.25, 0.1, 0.0}	0.67	0.62	0.60	0.44	0.93	0.76
{0.25, −0.1, 0.0}	0.89	0.82	0.77	0.61	1.30	1.06
{−0.25, 0.0, 0.0}	0.78	0.78	0.66	0.57	1.12	1.07
T300/5208						
{0.25, 0.0, 0.0}	0.76	0.69	0.64	0.50	1.09	0.86
{0.25, 0.1, 0.0}	0.65	0.59	0.59	0.42	0.91	0.72
{0.25, −0.1, 0.0}	0.86	0.78	0.75	0.58	1.27	1.00
{−0.25, 0.0, 0.0}	0.76	0.77	0.64	0.55	1.09	1.08

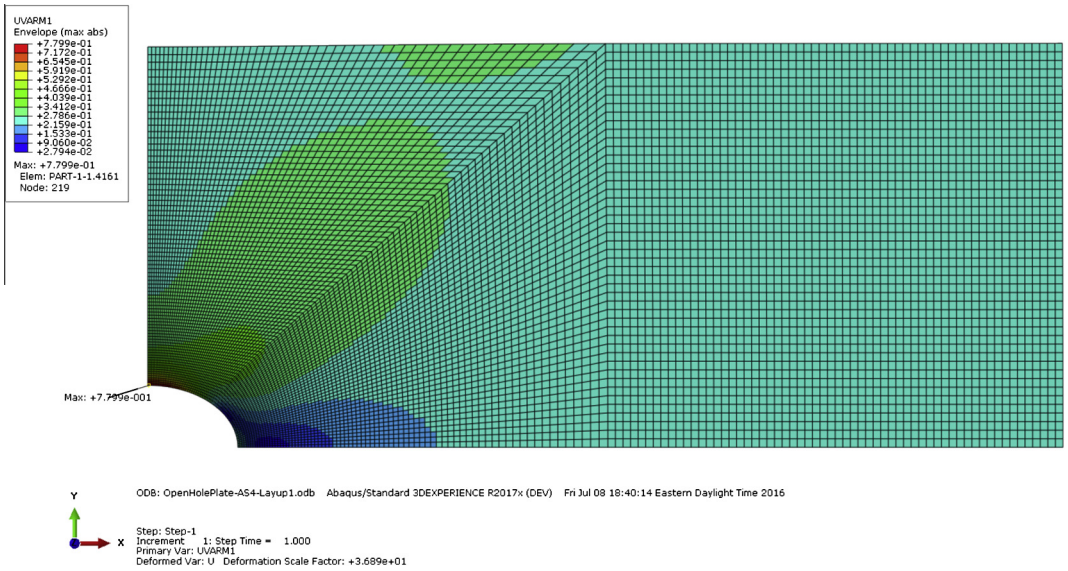

Fig. 8. Contour plot of failure index (k) of AS4/H3501 $[0/\pm45/90]_{2s}$ for load case {0.25, 0.0, 0.0} based on unit circle.

is defined geometrically according to ply angles, percentages, and stacking sequence. The optimized solution using master ply applies to laminates made of any UD CFRP. Thus, material selection comes later in design and trace is the only material property needed as the scaling factor for the determination of strains. For laminates with open hole, stress concentration factors can also be determined using master ply properties, thus valid for any CFRP. Failure analyses using FEA for open hole CFRP laminates considering various load cases indicated that the unit circle failure criterion is more conservative than Tsai-Wu. Thus, the calculation can be greatly simplified if the unit circle failure criterion is used since longitudinal tensile and compressive strengths, in addition to the longitudinal elastic modulus, are the only material properties required. In summary, the results presented in this work show that the invariant-based design approach, based on a reduced number of material properties, greatly simplifies the design procedure of CFPR structural components.

References

[1] Tsai SW, Wu EM. A general theory of strength for anisotropic materials. J Compos Mater 1971;5:58–80.
[2] Li L, Volovoi V, Hodges DH. Cross-sectional design of composite rotor blades. J Am Helicopter Soc 2008;53(3):240–51.
[3] Blasques JP, Stolpe M. Maximum stiffness and minimum weight optimization of laminated composite beams using continuous fiber angles. Struct Multidisc Optimiz 2011;43(4):573–88.
[4] Ganguli R, Chopra I. Aeroelastic optimization of a helicopter rotor with composite coupling. J Aircraft 1995;32(6):1326–34.
[5] Murugan S, Ganguli R. Aeroelastic stability enhancement and vibration suppression in a composite helicopter rotor. J Aircraft 2005;4:1013–24.
[6] Browne PA, Budd C, Gould NIM, Kim HA, Scott JA. A fast method for binary programming using first-order derivatives, with application to topology optimization with buckling constraints. Int J Numer Meth Eng 2012;92:1026–43.
[7] Park WJ. An optimal design of simple symmetric laminates under the first ply failure criteria. Wright-Patterson Air Force Base, Dayton OH: Materials Laboratory, Air Force Wright Aeronautical Laboratories, Air Force Systems Command; 1982. Report no. AFWAL-TR-81-4175.
[8] Fine AS, Springer GS. Design of composite laminates for strength, weight and manufacturability. J Compos Mater 1997;31(23):2330–90.
[9] Manne PM, Tsai SW. Design optimization of composite plates: part II – structural optimization by plydrop tapering. J Compos Mater 1998;32(6):544–71.
[10] Kim J-S, Kim C-G, Hong C-S. Optimum design of composite structures with ply drop using genetic algorithm and expert system shell. Compos Struct 1999;46:171–87.
[11] Kristinsdottir BP, Zabinsky ZB, Tuttle ME, Neogi E. Optimal design of large composite panels with varying loads. Compos Struct 2001;51:93–102.
[12] Pelletier JL, Vel SS. Multi-objective optimization of fiber reinforced composite laminates for strength, stiffness and minimal mass. Comput Struct 2006;84:2065–80.
[13] Zehnder N, Ermanni P. A methodology for the global optimization of laminated composite structures. Compos Struct 2006;72:311–20.

[14] Akbulut M, Sonmez FO. Design optimization of laminated composites using a new variant of simulated annealing. Comput Struct 2011;89:1712–24.
[15] Khot NS. Computer program (OPTCOMP) for optimization of composite structures for minimum weight design. Wright-Patterson Air Force Base, Ohio: Air Force Flight Dynamics, Air Force Wright Aeronautical, Air Force Systems Command; 1977. Technical Report AFFDL-TR-76-149.
[16] Miravete A. Optimization of laminated composite plates. Wright-Patterson Air Force Base, Dayton OH: Materials Laboratory, Air Force Wright Research and Development Center, Air Force Systems Command; 1989. Report no. WRDC-TR-89-4107.
[17] Assie AE, Kabeel AM, Mahmoud FF. Optimum design of laminated composite plates under dynamic excitation. Appl Math Model 2012;36:668–82.
[18] Walker M, Adali S, Verijenko V. Optimization of symmetric laminates for maximum buckling load including the effects of bending-twisting coupling. Comput Struct 1996;58(2):313–9.
[19] Kim CW, Hwang W, Park HC, Han KS. Stacking sequence optimization of laminated plates. Compos Struct 1997;39(3–4):283–8.
[20] Duvaut G, Terrel G, Léné F, Verijenko VE. Optimization of fiber reinforced composites. Comput Struct 2000;48:83–9.
[21] Park JH, Hwang JH, Lee CS, Hwang W. Stacking sequence design of composite laminates for maximum strength using genetic algorithms. Compos Struct 2001;52:217–31.
[22] Narita Y. Layerwise optimization for the maximum fundamental frequency of laminated composite plates. J Sound Vib 2003;263:1005–16.
[23] Stegmann J, Lund E. Discrete material optimization of general composite shell structures. Int J Numer Meth Eng 2005;62:2009–27.
[24] Irisarri F-X, Bassir DH, Carrere N, Maire J-F. Multiobjective stacking sequence optimization for laminated composite structures. Compos Sci Technol 2009;69:983–90.
[25] Keller D. Optimization of ply angles in laminated composite structures by a hybrid, asynchronous, parallel evolutionary algorithm. Compos Struct 2010;92:2781–90.
[26] Ersoy H. Optimum laminate design by using singular value decomposition. Composites Part B Eng 2013;52:144–54.
[27] Kogiso N, Watson LT, Gürdal Z, Haftka RT. Genetic algorithms with local improvement for composite laminate design. Struct Optim 1994;7:207–18.
[28] Liu B, Haftka RT, Akgün MA, Todoroki A. Permutation genetic algorithm for stacking sequence design of composite laminates. Comput Method Appl Mech Eng 2000:357–72.
[29] Lin C-C, Lee Y-J. Stacking sequence optimization of laminated composite structures using genetic algorithm with local improvement. Compos Struct 2004;63:339–45.
[30] Tsai SW, Melo JDD. An invariant-based theory of composites. Compos Sci Technol 2014;100:237–43.
[31] Tsai SW, Melo JDD. A unit circle failure criterion for carbon fiber reinforced polymer composites. Compos Sci Technol 2016;123:71–8.
[32] Tsai SW, Melo JDD. Composite materials design and testing. Stanford: Composites Design Group; 2015.
[33] Lekhnitskii SG. Anisotropic plates. third ed. Gordon and Breach Science Publishers; 1987.
[34] Camanho PP, Ercin GH, Catalanotti G, Mahdi S, Linde P. A finite fracture mechanics model for the prediction of the open-hole strength of composite laminates. Composites Part A 2012;43:1219–25.
[35] Ercin GH, Camanho PP, Xavier J, Catalanotti G, Mahdi S, Linde P. Size effects on the tensile and compressive failure of notched composite laminates. Compos Struct 2013;96:736–44.